

## **4. DATA REPORT: INORGANIC GEOCHEMISTRY AND MINERALOGY OF THE CRETACEOUS/TERTIARY BOUNDARY SECTION IN HOLE 1049C<sup>1</sup>**

C.D. Speed<sup>2</sup> and D. Kroon<sup>3</sup>

### **ABSTRACT**

Inorganic geochemistry and mineralogy of Core 171B-1049C-8X, containing a Cretaceous/Tertiary boundary section, was investigated by X-ray fluorescence (XRF) and X-ray diffraction (XRD). The ages of samples analyzed stretched from the latest Maastrichtian into the Danian. XRD measurements were made using the peak height method. A reduction in low-magnesium calcite and an increase in quartz were found above the spherule layer. Substantial amounts of dolomite were noted just above the spherule layer. XRF analyses were performed using the RHSMALL program to measure the abundance of major and minor elements. Replicate analyses for each technique were performed to assess the precision of the results. The section above the spherule bed was found to be characterized by peaks in many elements, including Si, Al, Fe, and Mg, as well as the following elemental ratios: Fe/Al, Ni/Al, Zr/Rb, and Rb/Sr'. Above the spherule bed, there were significant reductions in Ca, Sr/Ca, Ti/Al, K/Al, Rb/Al, Cr/Al, Ba/Al, biogenic Ba, and excess P.

### **INTRODUCTION**

The core to be analyzed in this study, Core 171B-1049C-8X, contains a well-preserved Cretaceous/Tertiary (K/T) boundary section (Shipboard Scientific Party, 1998). Above the boundary, the Danian sediments con-

<sup>1</sup>Speed, C.D., and Kroon, D., 2000. Data report: Inorganic geochemistry and mineralogy of the Cretaceous/Tertiary boundary section in Hole 1049C. *In* Kroon, D., Norris, R.D., and Klaus, A. (Eds.), *Proc. ODP, Sci. Results*, 171B, 1–26 [Online]. Available from World Wide Web: <[http://www-odp.tamu.edu/publications/171B\\_SR/VOLUME/CHAPTERS/SR171B04.PDF](http://www-odp.tamu.edu/publications/171B_SR/VOLUME/CHAPTERS/SR171B04.PDF)>. [Cited YYYY-MM-DD]

<sup>2</sup>School of Ocean and Earth Science, Southampton Oceanography Centre, European Way, Empress Dock, Southampton SO14 3ZH, United Kingdom. [cds1@mail.soc.soton.ac.uk](mailto:cds1@mail.soc.soton.ac.uk)

<sup>3</sup>Department of Geology and Geophysics, The University of Edinburgh, Grant Institute, West Mains Road, Edinburgh EH9 3JW, United Kingdom.

Initial receipt: 15 June 1999

Acceptance: 13 March 2000

Web publication: 15 September 2000  
Ms 171BSR-117

sist of white nannofossil ooze or chalk. This is separated from the underlying Maastrichtian gray nannofossil ooze by an olive-green impact-spherule bed comprised mostly of clay. This is interpreted as containing ejecta debris from the Chicxulub (northern Yucatan) impact, which slumped or flowed into deeper water following deposition (Bellier et al., 1997).

The inorganic geochemistry of the sediment was investigated to provide information about sedimentology and paleoproductivity of the K/T section. Mineralogical data is provided to help account for changes in inorganic geochemistry.

## METHODS

Samples 171B-1049C-8X-1, 2–4 cm, to 171B-1049C-8X-5, 126–128 cm, were received as dried and sieved sediment of <40- $\mu$ m grain size. Of the 107 samples analyzed, 104 were of Danian age, taken from above the spherule layer, and 3 were of latest Maastrichtian age, taken from below the spherule layer. The spherule layer was not analyzed in this study.

The samples were analyzed using X-ray diffraction (XRD) to determine which mineral phases were present. Samples were prepared by grinding a spatula-full of sample with acetone using a pestle and mortar. Six drops of this were transferred with a pipette onto a glass slide for analysis. Each sample was run over a period of 50 min. Peak heights associated with a particular mineral were measured.

This XRD method was used instead of using nonoriented powders because of the limited quantity of sediment available per sample. For this reason, neither acid digestion nor flotation could be used to determine the abundance of aluminosilicate minerals; therefore, these were not measured because of the difficulty in distinguishing the peaks from background values and deciphering cumulative peaks.

Precision data were collected for XRD by making three preparations of Sample 171B-1049C-8X-5, 106–108 cm, and running them separately. The results representing both instrumental precision and sample preparation precision are presented in Table T1. Standard errors were used to plot error bars on depth plots. Although accuracy data for the XRD analysis vary depending on the number of minerals present in a sample, for a two- or three-component sample, the accuracy has been estimated at  $\pm 10\%$  of the result for each component.

Abundance of minerals (in weight percent) was calculated from XRD data (Table T2) using Equation 1 and plotted against core depth (Fig. F1):

$$\text{Abundance of mineral (in weight percent)} = \frac{\text{corrected number of counts of mineral}}{\text{total corrected counts}} \times 100, \quad (1)$$

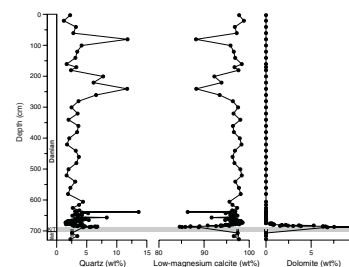
where corrected numbers of counts of minerals = counts of mineral/correction factor (quartz = 121.68; low-magnesium calcite = 68.87; dolomite = 58.82; from Alexander, 1996).

Elemental composition of the sediment samples was determined by X-ray fluorescence (XRF). For each sample, 3.00 g of dry sediment was hydraulically pressed (9 t of pressure for 2 min) into a pellet surrounded by boric acid ( $\text{H}_3\text{BO}_3$ ) powder. Some samples in the 630- to 680-cm high-resolution interval had to be combined to provide sufficient mate-

T1. Instrumental and sample preparation precision figures for Sample 171B-1049C-8X-5, 106–108 cm, p. 14.

T2. XRD data for Core 171B-1049C-8X, p. 15.

F1. Plot of mineralogy of Core 171B-1049C-8X, p. 7.



rial. Sample pellets were run sequentially, using the RHMALL program, to measure the abundance of major and minor elements.

The level of instrumental precision for XRF was investigated by running five replicate analyses (Tables T3, T4). From this, standard errors were used to plot error bars for depth curves. However, sample preparation precision could not be investigated as sufficient sample material was not available to make pressed pellets for replicates. Precision for major elements is considered to be better than accuracy, and vice-versa for minor elements. Accuracy data were unavailable for pressed pellet samples run on RHMALL.

Manganese was found to have variation less than its level of combined precision and accuracy because of its steplike curve, so it can be considered a low, invariant concentration. The variation of combined precision for other elements is believed to be lower than the variation of elemental abundance, as a steplike trend is not present.

Major element raw data are given in Table T5. XRF data were calculated according to the following equation:

$$\text{Weight percent element} = \frac{[(\text{weight percent oxide} \times \text{correction factor})/100]}{(2)}$$

Calculated values are presented on an oxide-free basis using the correction factors given in Table T6, and the abundance of each element was plotted against core depth (Tables T7, T8; Figs. F2, F3, F4).

Elemental abundances normalized against Al abundance are presented in Table T9 and plotted with depth in Figures F5 and F6. Other elemental ratios are presented in Table T10 and Figure F7. In addition to the Ba/Al ratio, the biogenic barium content of the sediment was calculated according to the normative relationship of Dymond et al., (1992):

$$\text{Ba}_{\text{bio}} = \text{Ba}_{\text{total}} - (\text{Al}_{\text{total}} \times \text{Ba}/\text{Al}_{\text{AS}}), \quad (3)$$

where  $\text{Ba}_{\text{bio}}$  is the biogenic barium mainly exported from surface waters,  $\text{Ba}_{\text{total}}$  is the concentration of barium measured by XRF,  $\text{Al}_{\text{total}}$  is the concentration of aluminium measured by XRF, and  $\text{Ba}/\text{Al}_{\text{AS}}$  is the lower limit of aluminosilicate barium (0.005) given in Dymond et al. (1992). This calculation corrects for the detrital component of barium, which had previously been measured in aluminosilicates.

Excess phosphorus was calculated according to Patience (1992):

$$\text{P}_{\text{ex}} = \text{P}_{\text{total}} - (\text{P}_{\text{pt}} + \text{P}_{\text{det}}), \quad (4)$$

where  $\text{P}_{\text{ex}}$  is the phosphorus not represented by a mineral phase,  $\text{P}_{\text{total}}$  is the concentration measured by XRF,  $\text{P}_{\text{pt}} = (\text{Y}_{\text{measured}} \times [26.9 \times 10^{-4}])$ , and  $\text{P}_{\text{det}}$  is detrital P from the world average shale ( $0.00875 \times \text{Al}$ ).

Rb/Sr' ratios were calculated using normalized calcium ( $\text{Ca}'$ ) to remove the component of strontium associated with carbonate material, from the desired aluminosilicate signature (S. Harley, pers. comm., 1998):

$$\text{Rb}/\text{Sr}' = (\text{Rb}/\text{Sr}) \times \text{Ca}', \quad (5)$$

T3. XRF major element precision figures for Sample 171B-1049C-8X-5, 88–90 cm, p. 17.

T4. XRF minor element precision figures for Sample 171B-1049C-8X-5, 88–90 cm, p. 18.

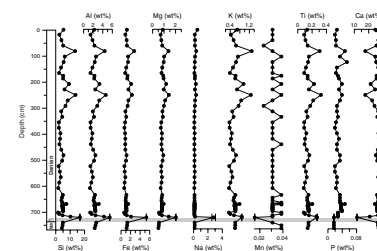
T5. Major element raw data from XRF analyses, p. 19.

T6. Correction factors of oxides to the weight percentage of elements, p. 20.

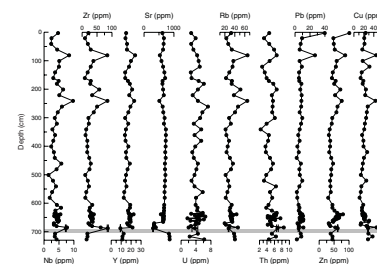
T7. Corrected major element abundance, p. 21.

T8. Minor element abundance, p. 22.

F2. Major element abundance with depth in Core 171B-1049C-8X, p. 8.



F3. Minor element abundance with depth in Core 171B-1049C-8X, p. 9.



where  $Ca' = (Ca_{\text{measured}}/Ca_{\text{normalized}}) \times Ca_{\text{measured}}$  is the weight percentage of Ca from XRF results and  $Ca_{\text{normalized}}$  is the average Ca percent value during “normal” Ca abundances (from Table T7).

## RESULTS

XRD results suggest that the dominant minerals present in the sediments are low-magnesium calcite and quartz (Fig. F1). Quartz and calcite curves were antithetic. Quartz shows larger peaks at 639- and 657-cm depth compared to 688.5 cm. Dolomite was present only in one interval, between 675.75 and 688.50 cm, with abundance decreasing upward.

Elements analyzed by XRF for the whole core show two opposing distribution patterns. First, Si, Al, Fe, Mg, Ti, Rb, Zr, Zn, Cu, Ni, Cr, and V show three main peaks of abundance at 81-, 241-, and 688-cm core depth (Figs. F2, F3, F4). Although aluminosilicate mineral abundance could not be measured by XRF, these elements suggest an increased abundance of clays at these intervals. Second, the curve for Ca and Sr shows the opposite trend with troughs at these core depths. Mn, U, Ba, Mo, and P shows curves that cannot be classified by these end-members.

The plots for major elements (Fig. F2) do not match the plots of mineralogy (Fig. F1) completely in interval 171B-1049C-8X-5, 60.0–60.5 cm, to 171B-1049C-8X-5, 87.5–88.0 cm, because samples were analyzed at a lower resolution for XRF because of the need for combining samples.

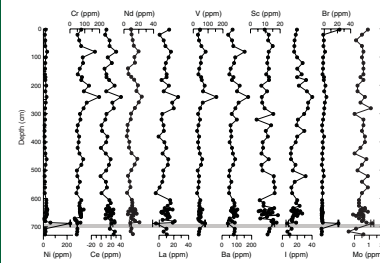
Redox sensitive metals (e.g., U, Ni, Zn, Cu, V, Cr, and Fe) (Patience, 1992) plotted for the whole core showed similar trends to those of Si (Figs. F3, F4). Fe was detected throughout the core ( $>1 \pm 0.032\%$ ) as  $Fe_2O_3$ , with a significant peak above the spherule layer. The plots of Zn/Al, Th/Al, U/Al, Cu/Al, Cr/Al, and V/Al (Figs. F5, F6) all show a similar trend of lowest values just above the spherule layer. Zn/Al and V/Al increase to a peak directly above these lowest values. This suggests that Zn, V, and Fe have been remobilized from the spherule layer and precipitated in the 18 cm above it. In the case of Fe, this has resulted in the orange-brown limonitic layer (Shipboard Scientific Party, 1998). Mn/Al was not plotted because the plot of Mn abundance with depth had variation less than its level of combined precision and accuracy. Pb/Al and Mo/Al ratios showed oscillating values throughout the core (Fig. F6).

K/Al and Rb/Al (Fig. F5) both show a decrease to the lowest values just above the spherule bed and have almost invariable values throughout the rest of the core. Mg/Al shows an increase in the value above the spherule bed, and above this, the ratio displays a similar curve to V/Al and Zn/Al.

Sr/Ca ratios plotted for the core show that Sr is present in calcium carbonate in varying amounts (Fig. F7). Sr/Ca ratios have been found to decrease with increasing diagenesis (Kinsman, 1969; Baker et al., 1982). Between 707 and 727 cm, Sr/Ca ratios are  $\sim 0.0032$ , whereas normal values above 665 cm are  $\sim 0.0025$ . There is a substantial reduction in the ratio at 670.5–685.25 cm to 0.00117, corresponding with the peak in Si. This is followed by a sudden return to normal values. The other two peaks in Si, however, were represented by peaks in Sr/Ca.

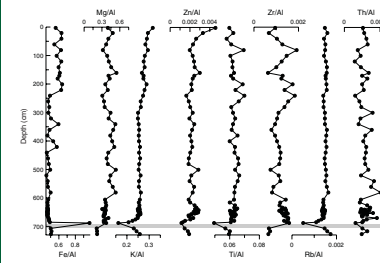
To detect any terrigenous material, the Rb/Sr', Ti/Al, Zr/Rb, and Cr/Zr ratios may be used (Patience, 1992). Ti/Al shows lowest values just above the spherule bed (Fig. F5). Using the Sr/Ca ratio, a Rb/Sr ratio cor-

F4. Minor element abundance with depth in Core 171B-1049C-8X, p. 10.

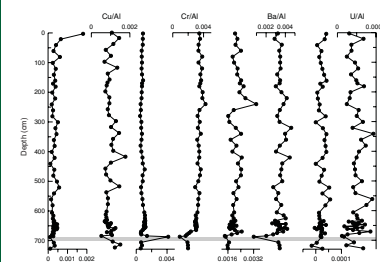


T9. Elemental abundances normalized against Al abundance, p. 24.

F5. Elemental abundances normalized against Al abundance, with depth in Core 171B-1049C-8X, p. 11.



F6. Elemental abundances normalized against Al abundance, with depth in Core 171B-1049C-8X, p. 12.



T10. Elemental ratios,  $Ba_{\text{bio}}$  and  $P_{\text{ex}}$  calculated from XRF data, p. 26.

rected for significant fluctuations in Ca was calculated. The plot of Rb/Sr' (Fig. F7) shows three main peaks in the ratio, which correspond to increases in Si concentration. The Zr/Rb record shows similar peaks, with the largest at 665.5–688.0 cm (Fig. F7). Ti/Al and Cr/Zr ratios used for proxies of sediment texture and degree of transport (Patience, 1992) showed the opposite trend above the spherule bed when compared to one another (Fig. F7). Zr/Al displays a sudden increase in value above the spherule layer and peaks at 61- and 221-cm depth (Fig. F5).

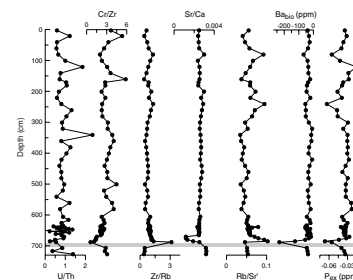
The concentration of biogenic Ba in marine sediments has been suggested to be a function of surface primary productivity (Dymond et al., 1992; Dehairs et al., 1991), particularly that associated with diatoms (Stroobants et al., 1991), and a function of preservation (Dymond et al., 1992). Preservation of biogenic Ba is enhanced by two main factors: (1) rapid accumulation rate which reduces the exposure of surface sediments to bottom waters that are undersaturated with respect to barium and (2) a greater barium-rain rate that increases the barium saturation of the sediment pore waters (Dymond et al., 1992). The Ba/Al (Fig. F6) and Ba<sub>bio</sub> (Fig. F7) show a noticeable decrease between 680.25 and 688.0 cm. In general, these plots oppose that of Si and resemble those of Zn/Al, Rb/Al, and V/Al. The values calculated for Ba<sub>bio</sub> were negative. This suggests that the Ba/Al<sub>AS</sub> ratio given by Dymond et al. (1992) was not applicable to the aluminosilicates in these sediments.

Patience (1992) suggested that phosphorus is an important constituent of organic matter, so it is potentially a useful indicator of paleoproductivity. P (Fig. F2) and P<sub>ex</sub> (Fig. F7) plotted with depth did not show similar curves to each other. P showed a peak at 121 cm and 639 cm, whereas P<sub>ex</sub> had a curve like that of Ca and Ba<sub>bio</sub>. The values calculated for P<sub>ex</sub> were negative because either the Y/P or P/Al correction factors (Patience, 1992) were not applicable to these sediments.

## ACKNOWLEDGMENTS

We thank the Ocean Drilling Program for providing sample material, Ian Alexander for helping with sample preparation and general advice, Dodie James for her help with the XRF, Geoff Angell and Trevor Clayton for with their instruction on XRD, Simon Harley for his help with ratioing and normalizing, Greg Cowie for advice on redox-sensitive elements, and James Casford for his proofreading of this manuscript.

**F7.** Elemental ratios, Ba<sub>bio</sub> and P<sub>ex</sub>, with depth in Core 171B-1049C-8X, p. 13.



## REFERENCES

- Alexander, I.T., 1996. Late Quaternary sedimentation off the Queensland continental margin (northeast Australia) in response to sea level fluctuations [Ph.D. thesis]. Edinburgh Univ., Edinburgh, Scotland.
- Baker, P.A., Gieskes, J.M., and Elderfield, H., 1982. Diagenesis of carbonates in deep-sea sediments: evidence from  $\text{Sr}^{2+}/\text{Ca}^{2+}$  ratios and interstitial dissolved  $\text{Sr}^{2+}$  data. *J. Sediment. Petrol.*, 52:71–82.
- Bellier, J.P., Marca, S., Norris, R.D., Kroon, D., Klaus, A., Alexander, I.T., Bardot, L.P., Barker, C.E., Blome, C.D., Clarke, L.J., Erbacher, J., Faul, K.L., Holmes, M.A., Huber, B.T., Katz, M.E., MacLeod, K.G., MartinezRuiz, F.C., Mita, I., Nakai, M., Ogg, J.G., Pak, D.K., Pletsch, T.K., SelfTrail, J.M., Shackleton, N.J., Smit, J., Ussler, W., Watkins, D.K., Widmark, J., and Wilson, P.A., 1997. The Blake Nose Cretaceous-Paleogene (Florida Atlantic margin, ODP Leg 171B): an exemplar record of the Maastrichtian-Danian transition. *C. R. Acad. Sci. Serie II: Sci. Terre Planetes*, 325:499–504.
- Dehairs, F., Stroobants, N., and Goeyens, L., 1991. Suspended barite as a tracer of biological activity in the Southern Ocean. *Mar. Chem.*, 35:399–410.
- Dymond, J., Suess, E., and Lyle, M., 1992. Barium in deep-sea sediment: a geochemical proxy for paleoproductivity. *Paleoceanography*, 7:163–181.
- Kinsman, D.J.J., 1969. Interpretation of  $\text{Sr}^{2+}$  concentrations in carbonate minerals and rocks. *J. Sediment. Petrol.*, 39:486–508.
- Patience, A.J., 1992. Geochemical indicators of palaeoproductivity and palaeoclimate in eastern equatorial Pacific Sediments [Ph.D. thesis]. Edinburgh Univ.
- Shipboard Scientific Party, 1998. Site 1049. In Norris, R.D., Kroon, D., Klaus, A., et al., *Proc. ODP, Init. Repts.*, 171B: College Station, TX (Ocean Drilling Program), 47–91.
- Stroobants, N., Dehairs, F., Goeyens, L., Vanderheijden, N., and Van Grieken, R., 1991. Barite formation in the Southern Ocean water column. *Mar. Chem.*, 35:411–421.

**Figure F1.** Plot of mineralogy of Core 171B-1049C-8X. The shaded area = the spherule layer, which overlies the K/T boundary (Shipboard Scientific Party, 1998). In the age scale, Mstr = the latest Maastrichtian.

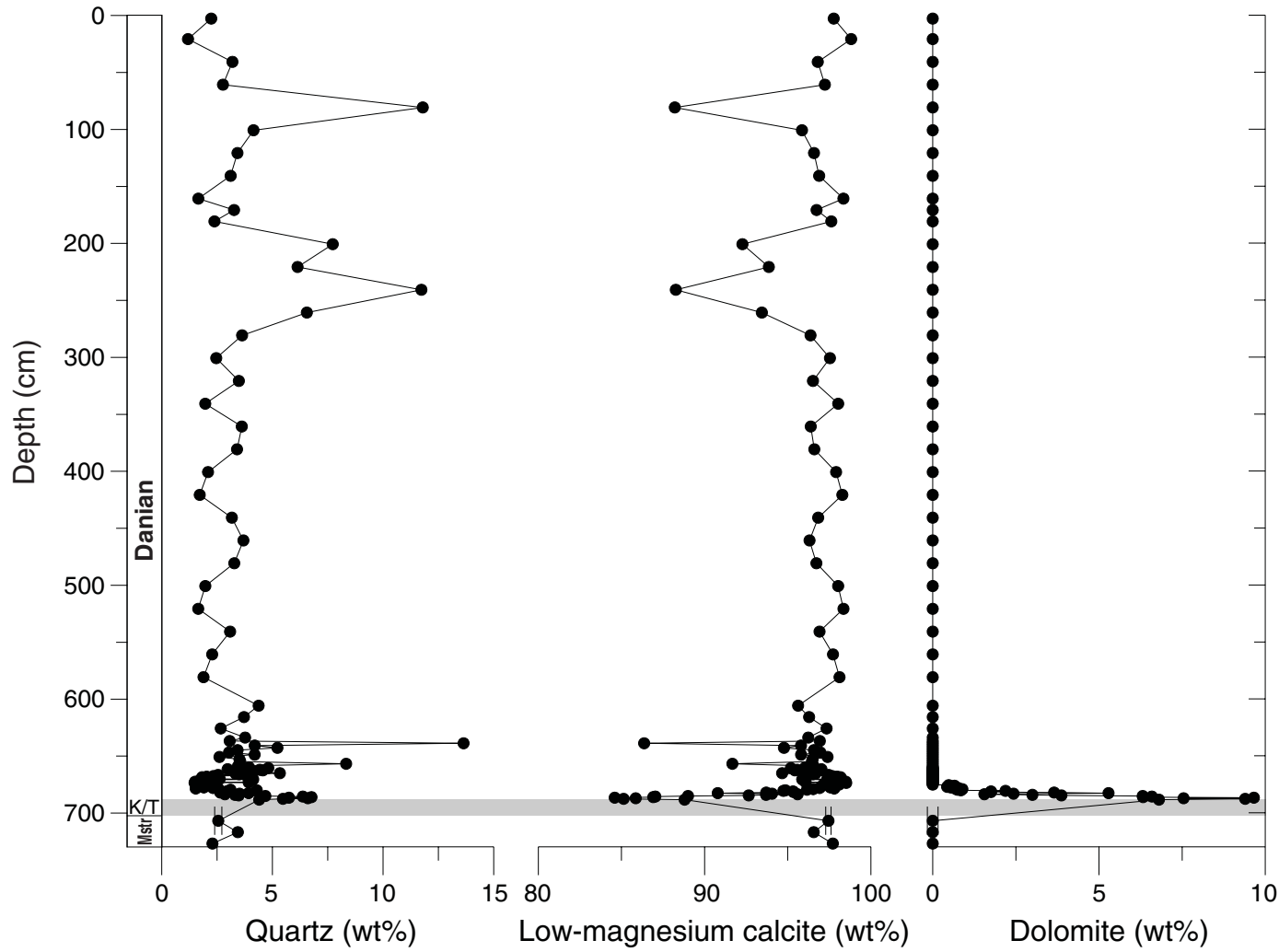


**Figure F2.** Major element abundance with depth in Core 171B-1049C-8X. The shaded area = the spherule layer, which overlies the K/T boundary (Shipboard Scientific Party, 1998). In the age scale, Mstr = the latest Maastrichtian.

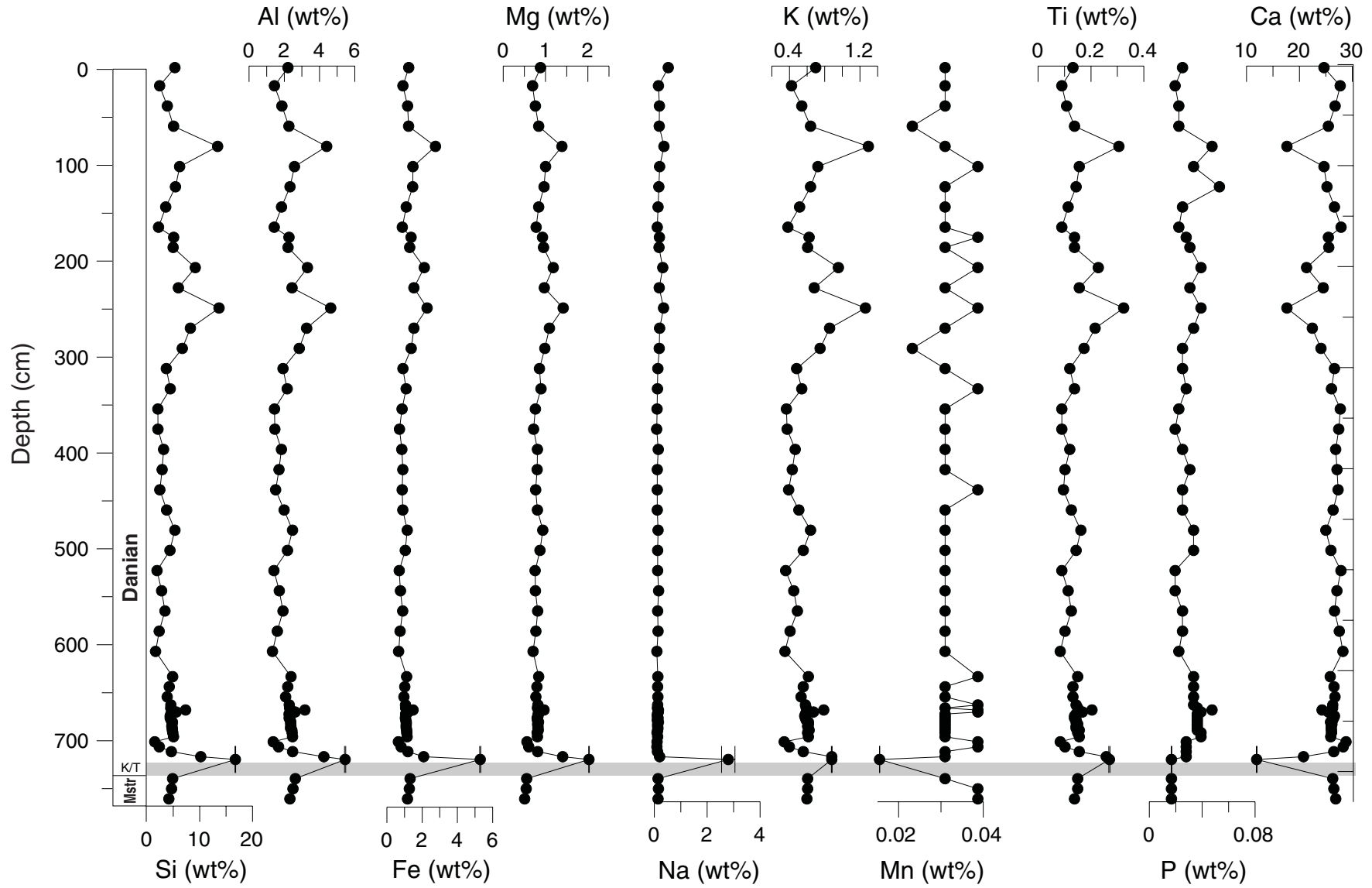




**Figure F3.** Minor element abundance with depth in Core 171B-1049C-8X. The shaded area = the spherule layer, which overlies the K/T boundary (Shipboard Scientific Party, 1998).

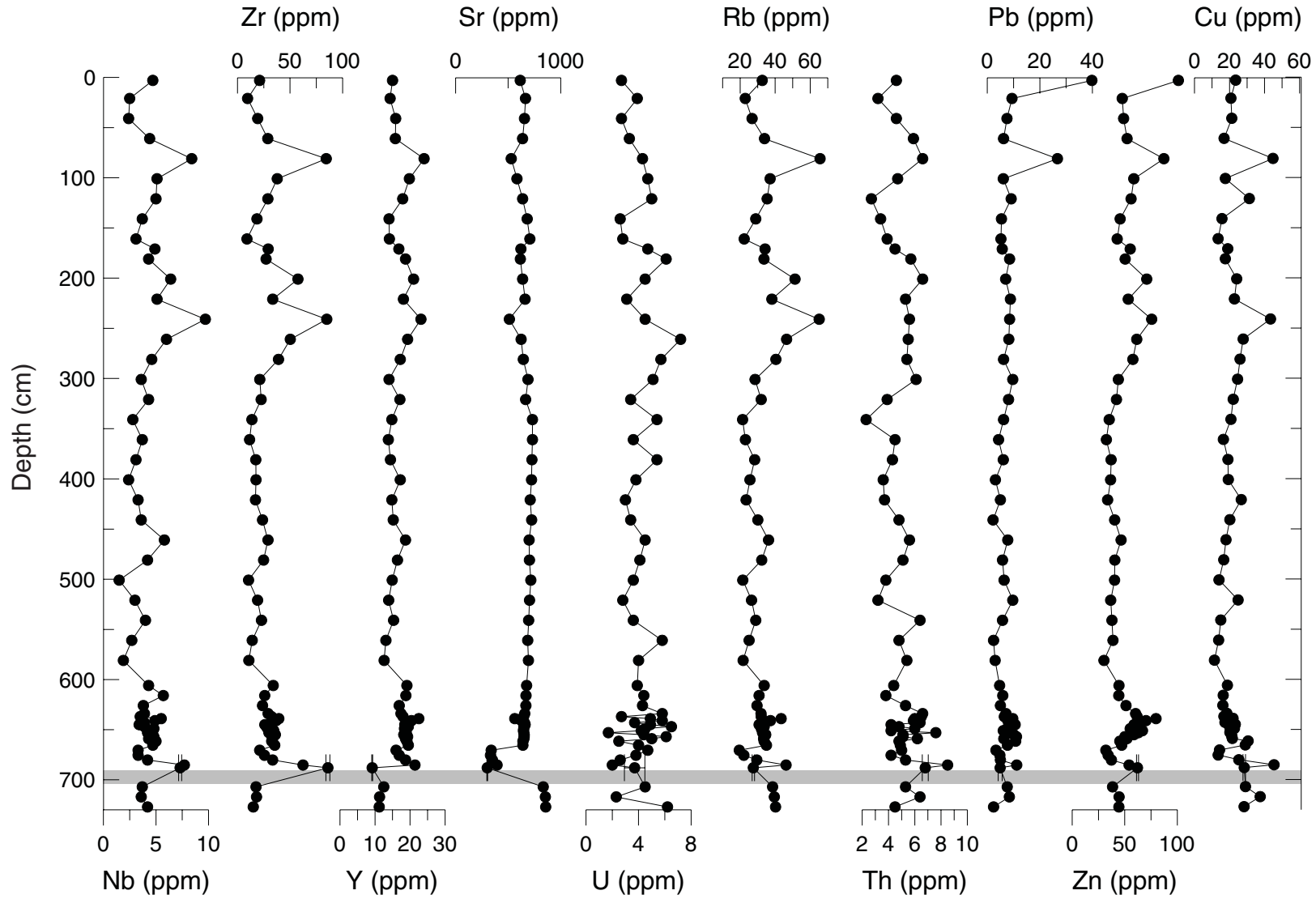
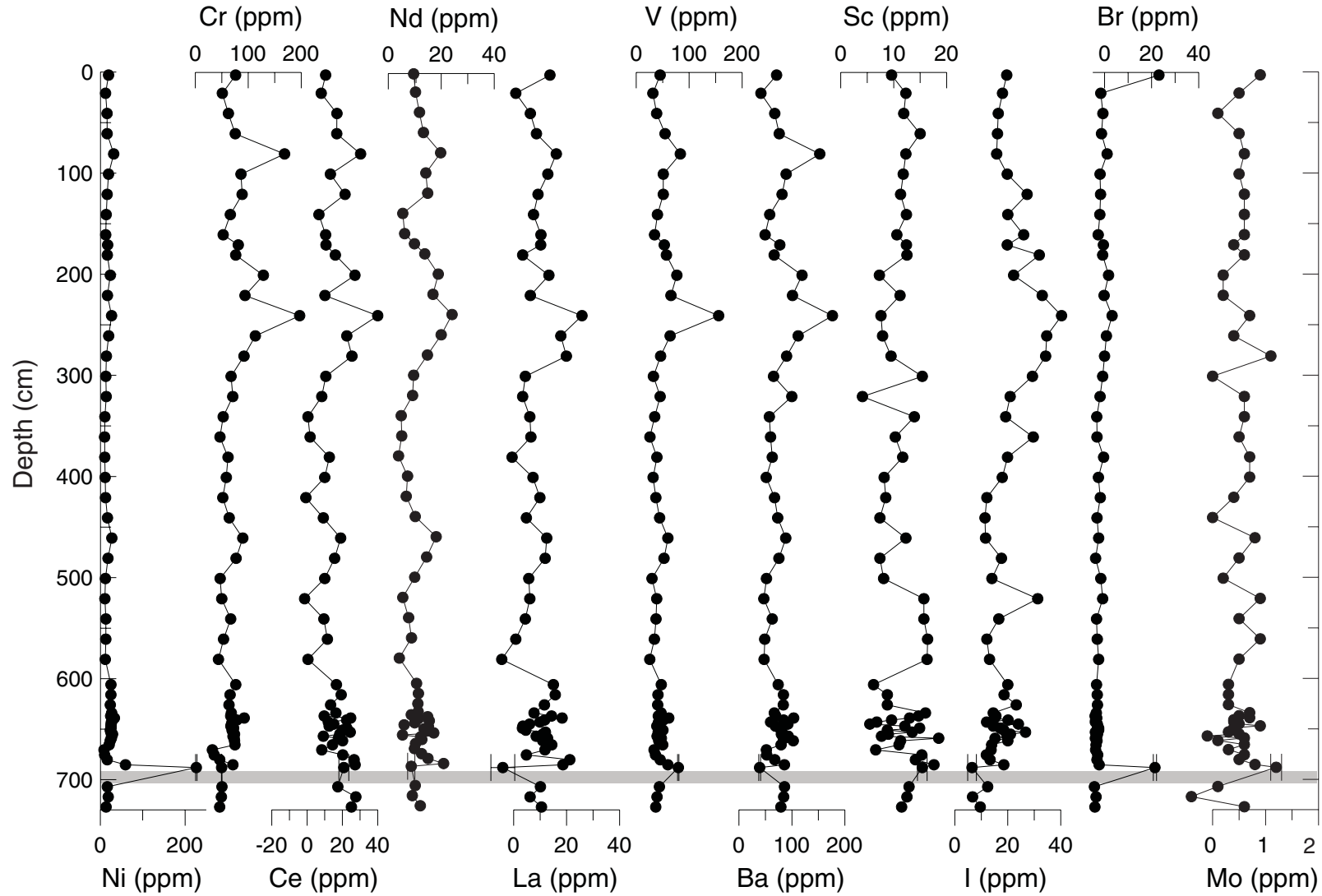
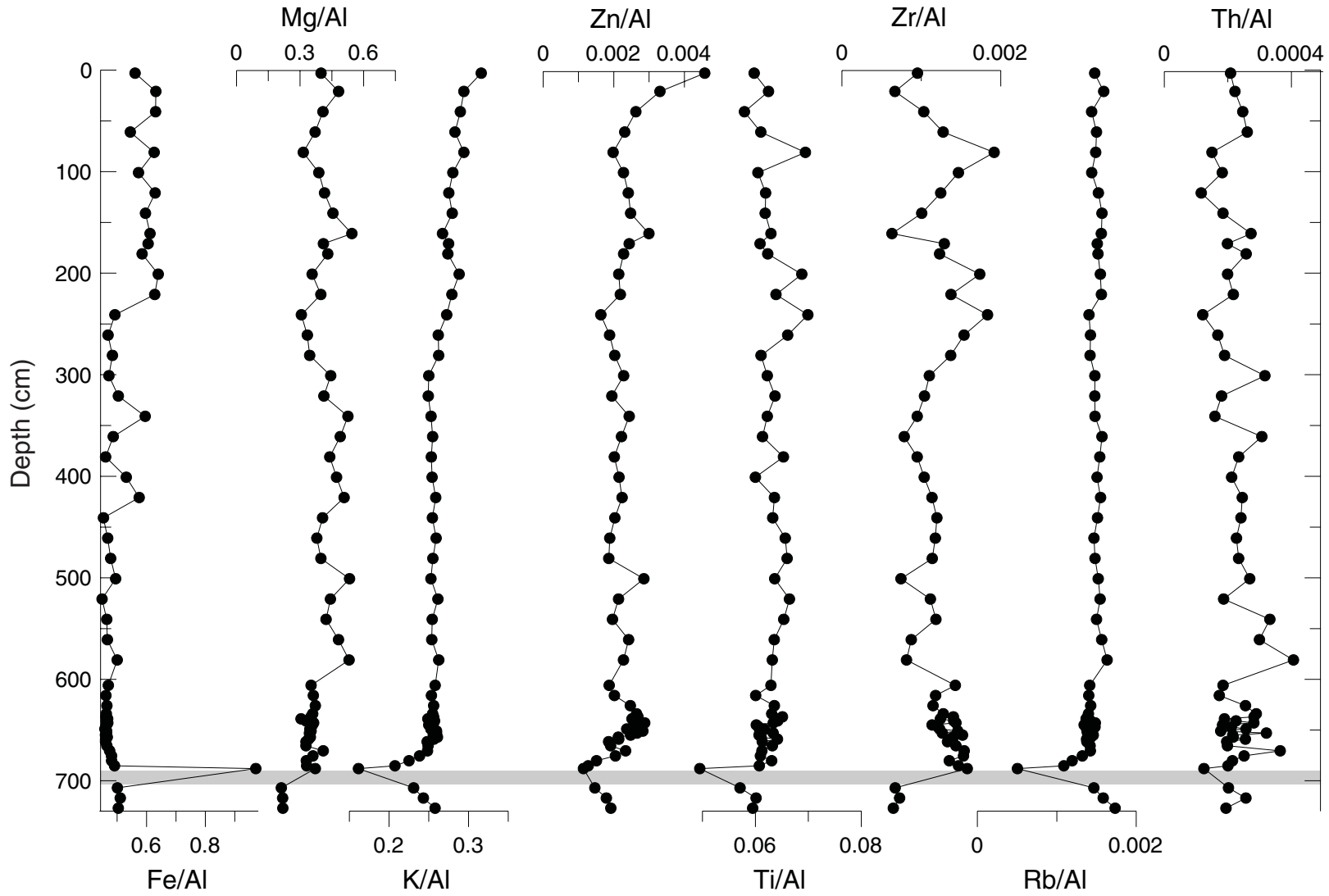


Figure F4. Minor element abundance with depth in Core 171B-1049C-8X. The shaded area = the spherule layer, which overlies the K/T boundary (Shipboard Scientific Party, 1998).



**Figure F5.** Elemental abundances normalized against Al abundance, with depth in Core 171B-1049C-8X. The shaded area = the spherule layer, which overlies the K/T boundary (Shipboard Scientific Party, 1998).



**Figure F6.** Elemental abundances normalized against Al abundance, with depth in Core 171B-1049C-8X. The shaded area = the spherule layer, which overlies the K/T boundary (Shipboard Scientific Party, 1998).

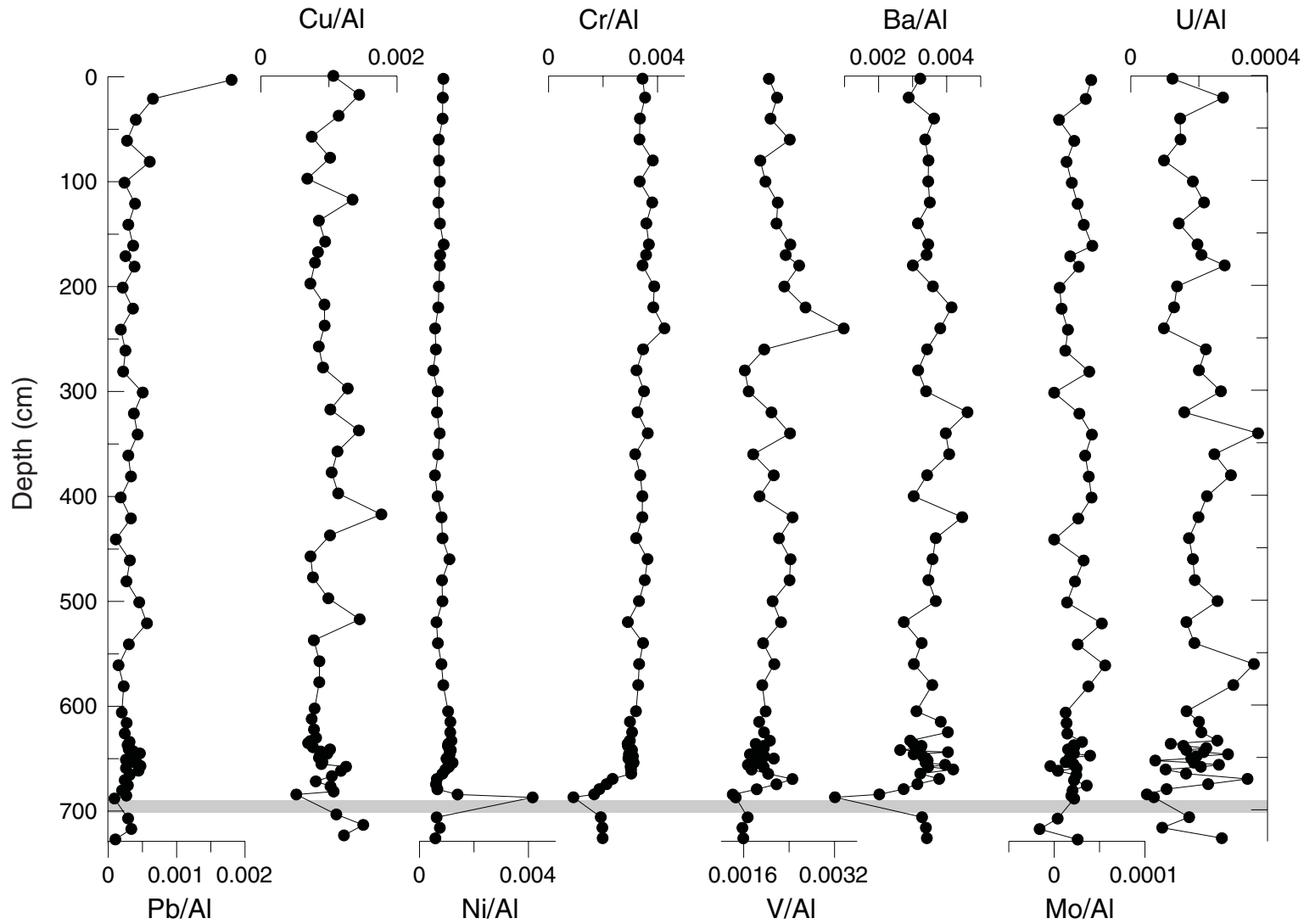


**Figure F7.** Elemental ratios,  $Ba_{bio}$  and  $P_{ex}$ , with depth in Core 171B-1049C-8X. The shaded area = the spherule layer, which overlies the K/T boundary (Shipboard Scientific Party, 1998).

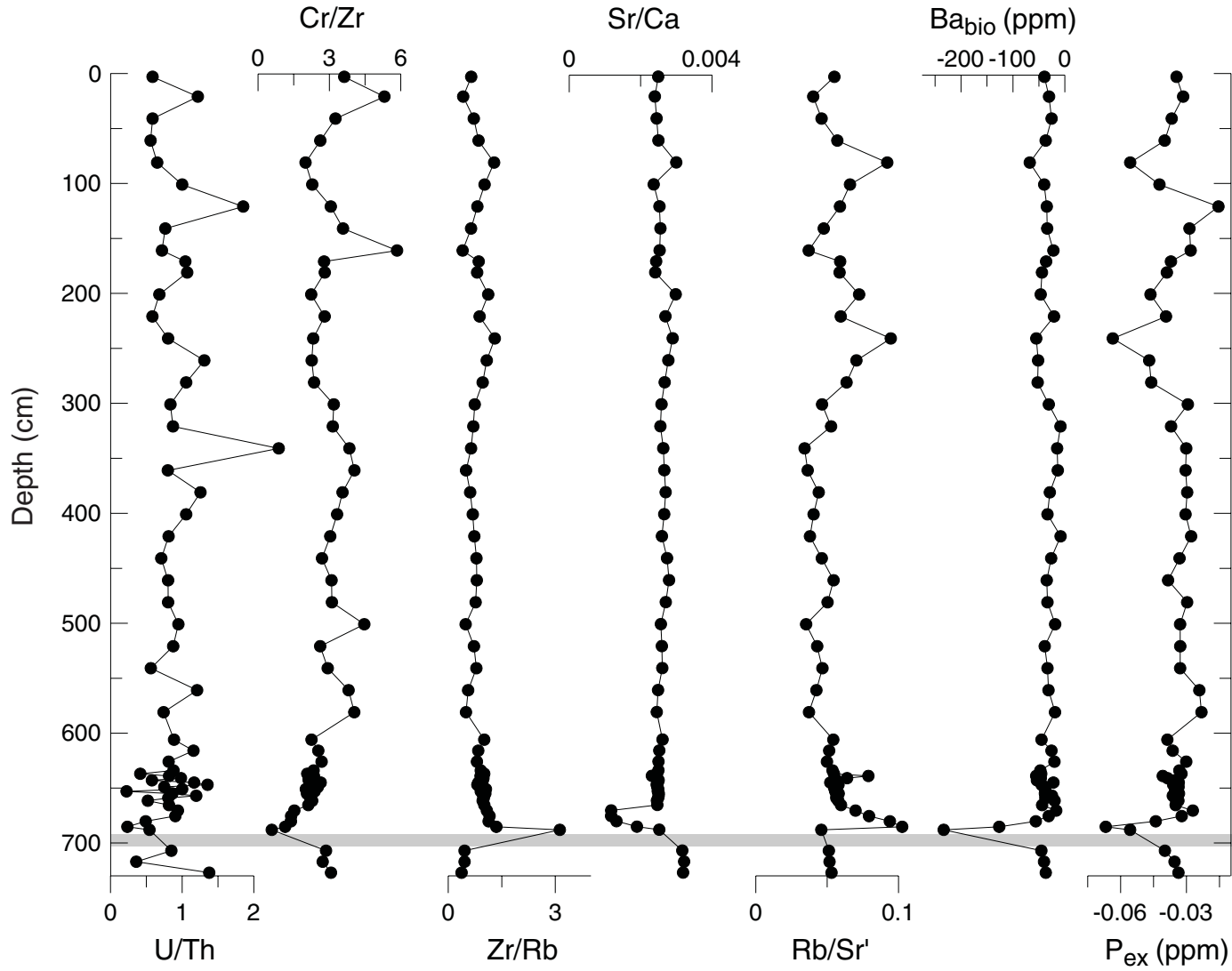


Table T1. Instrumental and sample preparation precision figures for three runs of Sample 171B-1049C-8X-5, 106–108 cm.

	Quartz (wt%)	Low-magnesium calcite (wt%)
Mean ( $N = 3$ )	4.222	95.778
Standard deviation*	0.277	0.277
Standard error	0.160	0.160
95% confidence	0.687	0.687
99% confidence	1.565	1.565

Note: \* = in standard deviation units; all other values are reported in weight percent.

Table T2. XRD data for Core 171B-1049C-8X. (See table note. Continued on next page.)

Core, section, interval (cm)	Depth (cm)	Quartz (counts)	Low- magnesium calcite (counts)	Dolomite (counts)	Total (counts)	Quartz (corrected)	Low- magnesium calcite (corrected)	Dolomite (corrected)	*Quartz (wt%)	*Low- magnesium calcite (wt%)	*Dolomite (wt%)
171B-1049C-											
8X-1, 2-4	3.00	306	7,552	0	7,858	3	110	0	2	98	0
8X-1, 20-22	21.00	177	8,317	0	8,494	1	121	0	1	99	0
8X-1, 40-42	41.00	600	10,262	0	10,862	5	149	0	3	97	0
8X-1, 60-62	61.00	488	9,683	0	10,171	4	141	0	3	97	0
8X-1, 80-82	81.00	1,482	6,257	0	7,739	12	91	0	12	88	0
8X-1, 100-102	101.00	524	6,839	0	7,363	4	100	0	4	96	0
8X-1, 120-122	121.00	522	8,317	0	8,839	4	121	0	3	97	0
8X-1, 140-142	141.00	576	10,120	0	10,696	5	147	0	3	97	0
8X-2, 10-12	161.00	228	7,656	0	7,884	2	111	0	2	98	0
8X-2, 20-22	171.00	502	8,391	0	8,893	4	122	0	3	97	0
8X-2, 30-32	181.00	372	8,608	0	8,980	3	125	0	2	98	0
8X-2, 50-52	201.00	1,102	7,430	0	8,532	9	108	0	8	92	0
8X-2, 70-72	221.00	829	7,157	0	7,986	7	104	0	6	94	0
8X-2, 90-92	241.00	1,197	5,084	0	6,281	10	74	0	12	88	0
8X-2, 110-112	261.00	1,082	8,705	0	9,787	9	127	0	7	93	0
8X-2, 130-132	281.00	576	8,630	0	9,206	5	126	0	4	96	0
8X-3, 0-4	301.00	420	9,390	0	9,810	3	137	0	2	98	0
8X-3, 20-22	321.00	462	7,225	0	7,687	4	105	0	3	97	0
8X-3, 40-42	341.00	361	10,161	0	10,522	3	148	0	2	98	0
8X-3, 60-62	361.00	708	10,650	0	11,358	6	155	0	4	96	0
8X-3, 80-82	381.00	581	9,312	0	9,893	5	136	0	3	97	0
8X-3, 100-102	401.00	400	10,568	0	10,968	3	154	0	2	98	0
8X-3, 120-122	421.00	266	8,593	0	8,859	2	125	0	2	98	0
8X-3, 140-142	441.00	566	9,761	0	10,327	5	142	0	3	97	0
8X-4, 10-12	461.00	480	7,073	0	7,553	4	103	0	4	96	0
8X-4, 30-32	481.00	566	9,428	0	9,994	5	137	0	3	97	0
8X-4, 50-52	501.00	346	9,722	0	10,068	3	142	0	2	98	0
8X-4, 70-72	521.00	193	6,496	0	6,689	2	95	0	2	98	0
8X-4, 90-92	541.00	376	6,659	0	7,035	3	97	0	3	97	0
8X-4, 110-112	561.00	365	8,836	0	9,201	3	129	0	2	98	0
8X-4, 130-132	581.00	328	9,624	0	9,952	3	140	0	2	98	0
8X-5, 5-7	606.00	575	7,090	0	7,665	5	103	0	4	96	0
8X-5, 15-17	616.00	681	9,960	0	10,641	6	145	0	4	96	0
8X-5, 25-27	626.00	493	10,161	0	10,654	4	148	0	3	97	0
8X-5, 33-35	634.00	713	10,282	0	10,995	6	150	0	4	96	0
8X-5, 36-38	637.00	396	7,056	0	7,452	3	103	0	3	97	0
8X-5, 38-40	639.00	2,098	7,500	0	9,598	17	109	0	14	86	0
8X-5, 40-42	641.00	576	7,413	0	7,989	5	108	0	4	96	0
8X-5, 42-44	643.00	515	5,271	0	5,786	4	77	0	5	95	0
8X-5, 44-46	645.00	595	9,467	0	10,062	5	138	0	3	97	0
8X-5, 46-48	647.00	408	7,344	0	7,752	3	107	0	3	97	0
8X-5, 48-50	649.00	784	10,100	0	10,884	6	147	0	4	96	0
8X-5, 50-52	651.00	412	8,686	0	9,098	3	126	0	3	97	0
8X-5, 52-54	653.00	600	9,312	0	9,912	5	136	0	4	96	0
8X-5, 54-56	655.00	538	8,263	0	8,801	4	120	0	4	96	0
8X-5, 56-58	657.00	1,136	7,056	0	8,192	9	103	0	8	92	0
8X-5, 58-60	659.00	502	7,939	0	8,441	4	116	0	3	97	0
8X-5, 60-60.5	660.25	534	7,327	0	7,861	4	107	0	4	96	0
8X-5, 60.5-61	660.75	635	7,090	0	7,725	5	103	0	5	95	0
8X-5, 61-61.5	661.25	557	7,797	0	8,354	5	114	0	4	96	0
8X-5, 61.5-62	661.75	471	8,668	0	9,139	4	126	0	3	97	0
8X-5, 62-62.5	662.25	524	6,384	0	6,908	4	93	0	4	96	0
8X-5, 62.5-63	662.75	740	8,724	0	9,464	6	127	0	5	95	0
8X-5, 63-63.5	663.25	600	8,742	0	9,342	5	127	0	4	96	0
8X-5, 63.5-64	663.75	702	9,216	0	9,918	6	134	0	4	96	0
8X-5, 64-64.5	664.25	557	9,044	0	9,601	5	132	0	3	97	0
8X-5, 64.5-65	664.75	615	8,780	0	9,395	5	128	0	4	96	0
8X-5, 65-65.5	665.25	751	7,517	0	8,268	6	109	0	5	95	0
8X-5, 65.5-66	665.75	576	9,409	0	9,985	5	137	0	3	97	0
8X-5, 66-66.5	666.25	625	9,742	0	10,367	5	142	0	3	97	0
8X-5, 66.5-67	666.75	384	8,299	0	8,683	3	121	0	3	97	0
8X-5, 67-67.5	667.25	605	8,612	0	9,217	5	125	0	4	96	0
8X-5, 67.5-68	667.75	372	8,780	0	9,152	3	128	0	2	98	0
8X-5, 68-68.5	668.25	365	9,940	0	10,305	3	145	0	2	98	0
8X-5, 68.5-69	668.75	272	8,263	0	8,535	2	120	0	2	98	0
8X-5, 69-69.5	669.25	380	10,899	0	11,279	3	159	0	2	98	0

**Table T2 (continued).**

Core, section, interval (cm)	Depth (cm)	Quartz (counts)	Low- magnesium calcite (counts)	Dolomite (counts)	Total (counts)	Quartz (corrected)	Low- magnesium calcite (corrected)	Dolomite (corrected)	*Quartz (wt%)	*Low- magnesium calcite (wt%)	*Dolomite (wt%)
8X-5, 69.5-70	669.75	400	10,774	0	11,174	3	157	0	2	98	0
8X-5, 70-70.5	670.25	493	10,343	0	10,836	4	151	0	3	97	0
8X-5, 70.5-71	670.75	801	10,486	0	11,287	7	153	0	4	96	0
8X-5, 71-71.5	671.25	279	8,949	0	9,228	2	130	0	2	98	0
8X-5, 71.5-72	671.75	380	8,968	0	9,348	3	131	0	2	98	0
8X-5, 72-72.5	672.25	420	11,968	0	12,388	3	174	0	2	98	0
8X-5, 72.5-73	672.75	196	7,225	0	7,421	2	105	0	2	98	0
8X-5, 73-73.5	673.25	807	11,151	0	11,958	7	162	0	4	96	0
8X-5, 73.5-74	673.75	317	11,881	0	12,198	3	173	0	1	99	0
8X-5, 74-74.5	674.25	421	11,385	0	11,806	3	166	0	2	98	0
8X-5, 74.5-75	674.75	458	11,428	0	11,886	4	166	0	2	98	0
8X-5, 75-75.5	675.25	361	10,445	0	10,806	3	152	0	2	98	0
8X-5, 75.5-76	675.75	493	11,278	48	11,819	4	164	1	2	97	0
8X-5, 76-76.5	676.25	416	10,040	58	10,514	3	146	1	2	97	1
8X-5, 76.5-77	676.75	361	10,795	61	11,217	3	157	1	2	98	1
8X-5, 77-77.5	677.25	328	9,467	36	9,831	3	138	1	2	98	0
8X-5, 77.5-78	677.75	299	8,668	41	9,008	2	126	1	2	98	1
8X-5, 78-78.5	678.25	324	7,656	52	8,032	3	111	1	2	97	1
8X-5, 78.5-79	678.75	289	10,384	61	10,734	2	151	1	2	98	1
8X-5, 79-79.5	679.25	454	9,604	76	10,134	4	140	1	3	97	1
8X-5, 79.5-80	679.75	600	10,486	69	11,155	5	153	1	3	96	1
8X-5, 80-80.5	680.25	756	9,428	72	10,256	6	137	1	4	95	1
8X-5, 80.5-81	680.75	529	9,197	182	9,908	4	134	3	3	95	2
8X-5, 81-81.5	681.25	557	10,221	161	10,939	5	149	3	3	95	2
8X-5, 81.5-82	681.75	493	9,139	144	9,776	4	133	2	3	95	2
8X-5, 82-82.5	682.25	346	6,922	231	7,499	3	101	4	3	94	4
8X-5, 82.5-83	682.75	671	8,761	437	9,869	6	128	7	4	91	5
8X-5, 83-83.5	683.25	610	9,216	204	10,030	5	134	3	4	94	2
8X-5, 83.5-84	683.75	445	8,409	117	8,971	4	122	2	3	96	2
8X-5, 84-84.5	684.25	520	8,317	228	9,065	4	121	4	3	94	3
8X-5, 84.5-85	684.75	576	8,664	310	9,550	5	126	5	3	93	4
8X-5, 85-85.5	685.25	595	6,384	388	7,367	5	93	7	5	89	6
8X-5, 85.5-86	685.75	824	6,352	412	7,588	7	93	7	6	87	7
8X-5, 86-86.5	686.25	876	6,352	396	7,624	7	93	7	7	87	6
8X-5, 86.5-87	686.75	645	5,358	524	6,527	5	78	9	6	85	10
8X-5, 87-87.5	687.25	702	5,155	388	6,245	6	75	7	7	86	8
8X-5, 87.5-88	687.75	552	4,844	458	5,854	5	71	8	5	85	9
8X-5, 88-90	688.50	400	4,556	299	5,255	3	66	5	4	89	7
8X-5, 106-108	707.00	445	9,584	0	10,029	4	140	0	3	97	0
8X-5, 116-118	717.00	462	7,327	0	7,789	4	107	0	3	97	0
8X-5, 126-128	727.00	445	10,712	0	11,157	4	156	0	2	98	0

Note: Depth refers to depth in Core 171B-1049C-8X. \* = reported weight percent values are rounded to the nearest percent.



Table T3. Major element precision figures for five XRF runs of Sample 171B-1049C-8X-5, 88–90 cm.

Element (wt%)	Mean (N = 5)	Standard deviation*	Standard error	95% confidence	99% confidence
Si	17.031	0.157	0.070	0.195	0.323
Al	5.575	0.071	0.032	0.088	0.146
Fe	5.420	0.071	0.032	0.089	0.147
Mg	2.055	0.018	$7.955 \times 10^{-3}$	0.022	0.037
Ca	12.141	0.127	0.057	0.158	0.262
Na	1.782	0.567	0.254	0.705	1.168
K	0.897	0.010	$4.547 \times 10^{-3}$	0.013	0.021
Mn	0.015	$7.276 \times 10^{-12}$	$3.254 \times 10^{-12}$	$9.034 \times 10^{-12}$	$1.498 \times 10^{-11}$
Ti	0.278	$5.362 \times 10^{-3}$	$2.398 \times 10^{-3}$	$6.658 \times 10^{-3}$	0.011
P	0.017	0.000	0.000	0.000	0.000

Note: \* = in standard deviation units; all other units are the same as elemental abundance.

**Table T4.** Minor element precision figures for five XRF runs of Sample 171B-1049C-8X-5, 88–90 cm.

Element (ppm)	Mean (N = 5)	Standard deviation*	Standard error	95% confidence	99% confidence
Nb	7.800	0.316	0.141	0.393	0.651
Zr	92.820	4.194	1.875	5.207	8.633
Y	9.580	0.268	0.120	0.333	0.552
Sr	308.720	8.574	3.834	10.645	17.649
U	5.160	1.742	0.779	2.162	3.585
Rb	29.380	1.499	0.670	1.861	3.086
Th	7.200	0.515	0.230	0.639	1.060
Pb	7.600	1.725	0.771	2.142	3.551
Zn	64.640	2.134	0.954	2.649	4.392
Cu	31.140	1.587	0.710	1.970	3.266
Ni	232.440	3.890	1.740	4.830	8.008
Cr	49.760	0.961	0.430	1.193	1.978
Ce	27.860	6.222	2.783	7.726	12.809
Nd	6.360	3.088	1.381	3.834	6.356
La	11.600	10.034	4.487	12.458	20.655
V	79.760	2.855	1.277	3.545	5.878
Ba	36.860	4.028	1.801	5.001	8.291
Sc	14.580	2.030	0.908	2.521	4.179
I	7.200	3.641	1.628	4.520	7.494
Br	19.220	1.506	0.673	1.869	3.099
Mo	1.540	0.230	0.103	0.286	0.474

Note: \* = in standard deviation units; all other units are the same as elemental abundance.

Table T5. Major element raw data from XRF analyses.

Core, section, interval (cm)	Depth (cm)	SiO <sub>2</sub> (%)	Al <sub>2</sub> O <sub>3</sub> (%)	Fe <sub>2</sub> O <sub>3</sub> (%)	MgO (%)	CaO (%)	Na <sub>2</sub> O (%)	K <sub>2</sub> O (%)	MnO (%)	TiO <sub>2</sub> (%)	P <sub>2</sub> O <sub>5</sub> (%)	Total (%)
171B-1049C-												
8X-1, 2	3.00	11.38	4.17	1.77	1.46	34.49	0.71	0.84	0.04	0.22	0.09	55.17
8X-1, 20	21.00	5.21	2.72	1.30	1.15	38.78	0.21	0.51	0.04	0.15	0.07	50.13
8X-1, 40	41.00	8.32	3.52	1.68	1.26	37.43	0.26	0.65	0.04	0.18	0.08	53.40
8X-1, 60	61.00	10.84	4.27	1.76	1.39	35.65	0.25	0.77	0.03	0.23	0.08	55.27
8X-1, 80	81.00	28.68	8.32	3.94	2.30	24.68	0.49	1.56	0.04	0.51	0.17	70.70
8X-1, 100	101.00	13.29	4.87	2.11	1.66	34.49	0.27	0.87	0.05	0.26	0.12	57.99
8X-1, 120	121.00	11.61	4.39	2.09	1.60	35.28	0.23	0.77	0.04	0.24	0.19	56.44
8X-1, 140	141.00	7.67	3.48	1.57	1.39	37.26	0.19	0.62	0.04	0.19	0.09	52.50
8X-2, 10	161.00	4.76	2.70	1.25	1.29	39.01	0.15	0.46	0.04	0.15	0.08	49.89
8X-2, 20	171.00	10.89	4.28	1.96	1.54	35.65	0.26	0.75	0.05	0.23	0.10	55.71
8X-2, 30	181.00	10.67	4.18	1.85	1.58	35.75	0.24	0.73	0.04	0.23	0.11	55.39
8X-2, 50	201.00	19.63	6.26	3.03	1.96	29.88	0.43	1.15	0.05	0.38	0.14	62.89
8X-2, 70	221.00	12.79	4.61	2.19	1.61	34.29	0.25	0.82	0.04	0.26	0.11	56.97
8X-2, 90	241.00	29.24	8.75	3.26	2.35	24.68	0.47	1.52	0.05	0.54	0.14	71.00
8X-2, 110	261.00	17.65	6.17	2.19	1.81	31.40	0.27	1.03	0.04	0.36	0.12	61.05
8X-2, 130	281.00	14.37	5.38	1.97	1.63	33.69	0.25	0.90	0.03	0.29	0.09	58.62
8X-3, 0	301.00	7.91	3.64	1.30	1.42	37.26	0.18	0.58	0.04	0.20	0.09	52.61
8X-3, 20	321.00	9.51	4.09	1.56	1.48	36.47	0.16	0.65	0.05	0.23	0.10	54.30
8X-3, 40	341.00	4.49	2.73	1.23	1.26	38.81	0.14	0.44	0.04	0.15	0.08	49.38
8X-3, 60	361.00	4.52	2.77	1.02	1.19	38.39	0.12	0.45	0.04	0.15	0.07	48.73
8X-3, 80	381.00	6.81	3.47	1.21	1.34	37.58	0.20	0.56	0.04	0.20	0.09	51.49
8X-3, 100	401.00	6.22	3.21	1.29	1.33	37.94	0.15	0.52	0.04	0.17	0.11	50.99
8X-3, 120	421.00	5.28	2.85	1.24	1.27	38.22	0.15	0.47	0.05	0.16	0.09	49.77
8X-3, 140	441.00	8.04	3.76	1.29	1.34	36.91	0.15	0.61	0.04	0.21	0.09	52.44
8X-4, 10	461.00	11.38	4.66	1.65	1.55	34.98	0.19	0.77	0.04	0.27	0.12	55.61
8X-4, 30	481.00	9.38	4.12	1.49	1.44	36.32	0.17	0.67	0.04	0.24	0.12	53.98
8X-4, 50	501.00	4.15	2.67	1.00	1.25	38.98	0.17	0.43	0.04	0.15	0.07	48.91
8X-4, 70	521.00	6.01	3.24	1.10	1.26	37.91	0.22	0.54	0.04	0.19	0.07	50.59
8X-4, 90	541.00	7.36	3.64	1.28	1.35	37.28	0.17	0.59	0.04	0.21	0.09	51.99
8X-4, 110	561.00	5.03	3.03	1.07	1.28	38.54	0.19	0.49	0.04	0.17	0.09	49.92
8X-4, 130	581.00	3.56	2.51	0.95	1.17	39.50	0.13	0.42	0.04	0.14	0.08	48.49
8X-5, 5	606.00	10.47	4.50	1.60	1.39	36.14	0.18	0.74	0.05	0.25	0.12	55.46
8X-5, 15	616.00	9.09	4.15	1.45	1.32	37.13	0.17	0.67	0.04	0.22	0.12	54.37
8X-5, 25	626.00	8.27	3.92	1.38	1.28	37.40	0.18	0.64	0.04	0.22	0.12	53.45
8X-5, 33	634.00	9.75	4.31	1.51	1.36	36.81	0.17	0.70	0.05	0.24	0.12	55.02
8X-5, 36	637.00	9.70	4.35	1.52	1.34	36.77	0.16	0.71	0.04	0.25	0.13	54.97
8X-5, 38	639.00	15.71	5.99	2.12	1.60	33.98	0.21	0.95	0.05	0.34	0.17	61.11
8X-5, 40	641.00	11.94	4.94	1.73	1.42	35.66	0.20	0.81	0.05	0.28	0.14	57.18
8X-5, 42	643.00	9.77	4.29	1.52	1.37	36.54	0.16	0.70	0.04	0.24	0.13	54.77
8X-5, 44	645.00	9.47	4.33	1.52	1.36	37.26	0.15	0.69	0.04	0.23	0.13	55.19
8X-5, 46	647.00	9.49	4.30	1.50	1.33	37.03	0.19	0.70	0.04	0.23	0.13	54.95
8X-5, 48	649.00	9.84	4.41	1.53	1.34	36.77	0.15	0.71	0.04	0.24	0.13	55.18
8X-5, 50	651.00	10.38	4.47	1.57	1.38	36.22	0.21	0.74	0.04	0.24	0.13	55.38
8X-5, 52	653.00	10.24	4.47	1.57	1.35	36.59	0.17	0.74	0.04	0.25	0.13	55.55
8X-5, 54	655.00	10.13	4.48	1.56	1.36	36.41	0.17	0.73	0.04	0.24	0.13	55.26
8X-5, 56	657.00	10.31	4.45	1.57	1.36	36.39	0.18	0.74	0.04	0.24	0.13	55.41
8X-5, 58	659.00	10.36	4.59	1.60	1.37	36.45	0.17	0.75	0.04	0.26	0.13	55.72
8X-5, 61	661.50	10.53	4.62	1.61	1.33	36.47	0.14	0.73	0.04	0.25	0.14	55.88
8X-5, 65	665.50	10.83	4.66	1.64	1.34	36.27	0.17	0.74	0.04	0.26	0.14	56.10
8X-5, 70	670.50	3.23	2.59	0.93	0.93	40.32	0.14	0.41	0.05	0.14	0.10	48.85
8X-5, 75	675.50	5.06	3.16	1.15	1.00	39.58	0.13	0.48	0.05	0.17	0.10	50.88
8X-5, 80	680.25	9.94	4.67	1.70	1.35	37.08	0.16	0.67	0.04	0.26	0.10	55.96
8X-5, 84.5	685.25	21.84	8.02	2.98	2.33	29.07	0.27	1.06	0.04	0.43	0.10	66.15
8X-5, 88	688.00	35.84	10.30	7.57	3.36	16.68	3.77	1.06	0.02	0.45	0.06	79.11
8X-5, 106	707.00	10.46	4.96	1.88	0.92	36.81	0.19	0.73	0.04	0.25	0.06	56.31
8X-5, 116	717.00	10.03	4.71	1.82	0.90	37.10	0.21	0.73	0.05	0.25	0.06	55.86
8X-5, 126	727.00	8.93	4.38	1.67	0.84	37.59	0.19	0.72	0.05	0.23	0.06	54.66

Note: Depth refers to depth in Core 171B-1049C-8X.

Table T6. Correction factors for converting the weight percentage of oxides to the weight percentage of elements.

Conversion	Correction factor
SiO <sub>2</sub> ⇒Si	46.74
Al <sub>2</sub> O <sub>3</sub> ⇒Al	52.92
Fe <sub>2</sub> O <sub>3</sub> ⇒Fe	69.94
MgO⇒Mg	60.31
CaO⇒Ca	71.47
Na <sub>2</sub> O⇒Na	74.19
K <sub>2</sub> O⇒K	83.02
MnO <sub>2</sub> ⇒Mn	77.45
TiO <sub>2</sub> ⇒Ti	59.95
P <sub>2</sub> O <sub>5</sub> ⇒P	27.91





**Table T8 (continued).**

Core, section, interval (cm)	Depth (cm)	Nb (ppm)	Zr (ppm)	Y (ppm)	Sr (ppm)	U (ppm)	Rb (ppm)	Th (ppm)	Pb (ppm)	Zn (ppm)	Cu (ppm)	Ni (ppm)	Cr (ppm)	Ce (ppm)	Nd (ppm)	La (ppm)	V (ppm)	Ba (ppm)	Sc (ppm)	I (ppm)	Br (ppm)	Mo (ppm)
8X-5, 65	665.50	4.7	35.4	19.5	639.8	4.0	35.0	4.9	7.7	47.1	29.0	20.7	74.8	14.4	9.8	14.4	50.1	79.5	11.0	13.9	-3.60	0.60
8X-5, 70	670.50	3.3	21.1	16.0	338.6	4.7	19.5	5.0	3.3	32.0	14.3	8.7	32.2	8.3	9.4	11.8	33.7	51.8	6.6	13.7	-3.80	0.30
8X-5, 75	675.50	3.3	25.6	16.9	331.8	3.8	22.1	4.2	4.8	34.2	13.5	10.1	35.6	20.2	12.1	4.8	36.4	52.5	15.3	11.9	-2.90	0.60
8X-5, 80	680.25	4.2	33.4	18.7	350.5	2.6	29.5	5.3	5.0	37.3	25.3	16.2	46.1	26.6	14.5	21.2	45.2	67.6	14.1	13.3	-3.20	0.50
8X-5, 84.5	685.25	7.7	62.3	21.4	394.1	2.0	46.2	8.5	11.2	54.1	45.4	59.3	71.0	27.2	20.4	18.6	59.7	85.8	17.6	18.5	-2.30	0.80
8X-5, 88	688.00	7.3	86.0	9.2	300.8	3.7	27.5	6.8	4.9	62.1	28.4	226.4	49.7	20.8	8.2	-4.1	79.5	39.1	15.4	6.5	21.4	1.20
8X-5, 106	707.00	3.7	17.6	12.5	833.4	4.5	38.5	5.3	7.6	38.4	29.1	16.5	50.3	17.4	9.7	10.1	43.8	86.0	12.9	12.4	-4.30	0.10
8X-5, 116	717.00	3.6	18.1	11.3	853.7	2.3	39.5	6.4	8.4	44.6	37.5	18.6	49.2	27.6	8.6	6.2	39.3	84.5	12.5	6.7	-3.60	-0.40
8X-5, 126	727.00	4.2	15.0	11.2	857.1	6.2	40.2	4.5	2.4	44.4	28.3	13.5	46.0	25.1	11.6	10.5	36.9	79.2	11.5	9.6	-4.10	0.60

Note: Depth refers to depth in Core 171B-1049C-8X.





Table T9 (continued).

Core, section, interval (cm)	Depth (cm)	Fe/Al	Mg/Al	K/Al	Zn/Al	Ti/Al	Zr/Al	Rb/Al	U/Al	Th/Al	Pb/Al	Cu/Al	Ni/Al	Cr/Al	V/Al	Ba/Al	Mo/Al
8X-5, 65	665.50	0.475	0.409	0.248	0.0019	0.0612	0.00154	0.00142	0.000343	0.000365	0.000241	0.00104	0.000635	0.00235	0.00246	0.00378	0.0000219
8X-5, 70	670.50	0.481	0.361	0.238	0.0023	0.0609	0.00153	0.00132	0.000227	0.000251	0.000287	0.00081	0.000604	0.00213	0.00218	0.00314	0.0000359
8X-5, 75	675.50	0.481	0.329	0.225	0.0020	0.0631	0.00135	0.00119	0.000105	0.000214	0.000202	0.00102	0.000656	0.00187	0.00183	0.00274	0.0000202
8X-5, 80	680.25	0.491	0.331	0.207	0.0015	0.0607	0.00147	0.00109	0.000047	0.000200	0.000264	0.00107	0.001397	0.00167	0.00141	0.00202	0.0000188
8X-5, 84.5	685.25	0.971	0.372	0.161	0.0013	0.0495	0.00158	0.00050	0.000068	0.000125	0.000090	0.00052	0.004154	0.00091	0.00146	0.00072	0.0000220
8X-5, 88	688.00	0.501	0.211	0.231	0.0011	0.0571	0.00067	0.00147	0.000171	0.000202	0.000290	0.00111	0.000629	0.00192	0.00167	0.00328	0.0000038
8X-5, 106	707.00	0.511	0.218	0.243	0.0015	0.0601	0.00073	0.00158	0.000092	0.000257	0.000337	0.00150	0.000746	0.00197	0.00158	0.00339	-0.0000160
8X-5, 116	717.00	0.504	0.219	0.258	0.0018	0.0595	0.00065	0.00173	0.000267	0.000194	0.000104	0.00122	0.000582	0.00198	0.00159	0.00342	0.0000259
8X-5, 126	727.00	0.504	0.219	0.258	0.0019	0.0595	0.00065	0.00173	0.000267	0.000194	0.000104	0.00122	0.000582	0.00198	0.00159	0.00342	0.0000259

Note: Depth refers to depth in Core 171B-1049C-8X.

Table T10. Elemental ratios, Ba<sub>bio</sub> and P<sub>ex</sub> calculated from XRF data.

Core, section, interval (cm)	Depth (cm)	U/Th	Cr/Zr	Zr/Rb	Sr/Ca	Ca'	Rb/Sr	Rb/Sr'	Ba <sub>bio</sub> (ppm)	P <sub>nt</sub> (ppm)	P <sub>diet</sub> (ppm)	P <sub>ex</sub> (ppm)
171B-1049C-												
8X-1, 2	3.00	0.587	3.62	0.64	0.00249	1.04	0.0530	0.0550	-39	0.0404	0.0193	-0.034540185
8X-1, 20	21.00	1.219	5.31	0.42	0.00240	1.17	0.0345	0.0402	-30	0.0385	0.0126	-0.03152496
8X-1, 40	41.00	0.587	3.26	0.72	0.00245	1.13	0.0409	0.0461	-26	0.0428	0.0163	-0.03674236
8X-1, 60	61.00	0.559	2.62	0.85	0.00250	1.07	0.0532	0.0571	-37	0.0425	0.0198	-0.039946235
8X-1, 80	81.00	0.652	2.00	1.29	0.00300	0.74	0.1240	0.0921	-68	0.0646	0.0385	-0.05563876
8X-1, 100	101.00	1.000	2.28	1.02	0.00237	1.04	0.0636	0.0660	-40	0.0533	0.0226	-0.042320535
8X-1, 120	121.00	1.852	3.06	0.82	0.00253	1.06	0.0555	0.0590	-35	0.0482	0.0203	-0.015449895
8X-1, 140	141.00	0.765	3.57	0.64	0.00256	1.12	0.0425	0.0476	-34	0.0377	0.0161	-0.02865514
8X-2, 10	161.00	0.718	5.84	0.40	0.00253	1.17	0.0316	0.0371	-22	0.0379	0.0125	-0.02810335
8X-2, 20	171.00	1.044	2.78	0.85	0.00244	1.07	0.0551	0.0591	-36	0.0452	0.0198	-0.03710054
8X-2, 30	181.00	1.070	2.81	0.81	0.00241	1.08	0.0546	0.0587	-44	0.0503	0.0194	-0.03895749
8X-2, 50	201.00	0.682	2.23	1.12	0.00298	0.90	0.0805	0.0724	-47	0.0565	0.0290	-0.04640293
8X-2, 70	221.00	0.585	2.80	0.88	0.00270	1.03	0.0577	0.0595	-21	0.0487	0.0213	-0.03934605
8X-2, 90	241.00	0.804	2.32	1.30	0.00290	0.74	0.1273	0.0946	-55	0.0621	0.0405	-0.063581875
8X-2, 110	261.00	1.309	2.26	1.08	0.00278	0.94	0.0746	0.0705	-51	0.0519	0.0286	-0.046995185
8X-2, 130	281.00	1.056	2.36	0.97	0.00267	1.01	0.0627	0.0636	-52	0.0463	0.0249	-0.04606109
8X-3, 0	301.00	0.836	3.18	0.74	0.00259	1.12	0.0414	0.0464	-31	0.0377	0.0169	-0.02939602
8X-3, 20	321.00	0.872	3.14	0.70	0.00255	1.10	0.0481	0.0527	-8	0.0460	0.0189	-0.037027745
8X-3, 40	341.00	2.348	3.84	0.64	0.00264	1.17	0.0293	0.0342	-15	0.0398	0.0126	-0.030125265
8X-3, 60	361.00	0.800	4.05	0.50	0.00266	1.16	0.0315	0.0364	-14	0.0371	0.0128	-0.030411485
8X-3, 80	381.00	1.256	3.55	0.61	0.00270	1.13	0.0390	0.0441	-29	0.0387	0.0161	-0.029684835
8X-3, 100	401.00	1.056	3.32	0.69	0.00266	1.14	0.0355	0.0405	-33	0.0463	0.0149	-0.030430905
8X-3, 120	421.00	0.811	3.04	0.73	0.00260	1.15	0.0330	0.0379	-8	0.0398	0.0132	-0.027889925
8X-3, 140	441.00	0.708	2.69	0.79	0.00274	1.11	0.0416	0.0462	-26	0.0409	0.0174	-0.03317968
8X-4, 10	461.00	0.804	3.09	0.80	0.00280	1.05	0.0518	0.0545	-35	0.0503	0.0216	-0.03838913
8X-4, 30	481.00	0.804	3.10	0.77	0.00271	1.09	0.0460	0.0503	-34	0.0441	0.0191	-0.02970166
8X-4, 50	501.00	0.947	4.47	0.49	0.00257	1.17	0.0300	0.0352	-19	0.0401	0.0124	-0.032907435
8X-4, 70	521.00	0.875	2.61	0.72	0.00260	1.14	0.0377	0.0430	-39	0.0374	0.0150	-0.03285682
8X-4, 90	541.00	0.563	2.93	0.79	0.00261	1.12	0.0416	0.0467	-33	0.0412	0.0169	-0.02983902
8X-4, 110	561.00	1.208	3.81	0.56	0.00249	1.16	0.0366	0.0425	-31	0.0352	0.0140	-0.024150415
8X-4, 130	581.00	0.741	4.05	0.50	0.00245	1.19	0.0313	0.0373	-19	0.0339	0.0116	-0.023188555
8X-5, 5	606.00	0.886	2.25	1.01	0.00261	1.09	0.0499	0.0543	-45	0.0514	0.0208	-0.03872425
8X-5, 15	616.00	1.158	2.53	0.84	0.00252	1.12	0.0460	0.0514	-26	0.0506	0.0192	-0.036296575
8X-5, 25	626.00	0.811	2.67	0.80	0.00250	1.13	0.0443	0.0498	-20	0.0455	0.0182	-0.03012056
8X-5, 33	634.00	0.879	2.34	0.91	0.00250	1.11	0.0485	0.0538	-47	0.0468	0.0200	-0.033271455
8X-5, 36	637.00	0.415	2.07	1.01	0.00246	1.11	0.0495	0.0547	-46	0.0484	0.0201	-0.032279675
8X-5, 38	639.00	0.817	2.35	0.91	0.00232	1.02	0.0771	0.0789	-55	0.0605	0.0277	-0.040814695
8X-5, 40	641.00	0.983	2.13	0.99	0.00246	1.07	0.0596	0.0640	-46	0.0549	0.0229	-0.03867667
8X-5, 42	643.00	0.578	2.13	0.97	0.00251	1.10	0.0515	0.0566	-54	0.0514	0.0199	-0.034960845
8X-5, 44	645.00	1.167	2.63	0.84	0.00248	1.12	0.0466	0.0522	-22	0.0498	0.0201	-0.033532065
8X-5, 46	647.00	1.354	2.44	0.82	0.00245	1.11	0.0520	0.0579	-45	0.0525	0.0199	-0.03608315
8X-5, 48	649.00	0.750	2.52	0.89	0.00247	1.11	0.0495	0.0548	-40	0.0495	0.0204	-0.033633505
8X-5, 50	651.00	1.000	2.01	1.06	0.00249	1.09	0.0507	0.0553	-38	0.0503	0.0207	-0.034718335
8X-5, 52	653.00	0.224	2.38	0.91	0.00248	1.10	0.0506	0.0557	-37	0.0508	0.0207	-0.035256335
8X-5, 54	655.00	0.863	2.06	1.04	0.00251	1.10	0.0530	0.0581	-38	0.0490	0.0207	-0.03341964
8X-5, 56	657.00	1.196	2.16	0.98	0.00251	1.10	0.0517	0.0566	-25	0.0519	0.0206	-0.036239725
8X-5, 58	659.00	0.806	2.20	1.00	0.00249	1.10	0.0514	0.0564	-38	0.0503	0.0213	-0.035273995
8X-5, 61	661.50	0.521	2.28	0.96	0.00246	1.10	0.0526	0.0578	-20	0.0514	0.0214	-0.03369791
8X-5, 65	665.50	0.816	2.11	1.01	0.00247	1.09	0.0547	0.0597	-44	0.0525	0.0216	-0.03495913
8X-5, 70	670.50	0.940	1.53	1.08	0.00118	1.21	0.0576	0.0699	-17	0.0430	0.0120	-0.027122995
8X-5, 75	675.50	0.905	1.39	1.16	0.00117	1.19	0.0666	0.0793	-31	0.0455	0.0146	-0.03218338
8X-5, 80	680.25	0.491	1.38	1.13	0.00132	1.12	0.0842	0.0939	-56	0.0503	0.0216	-0.044017435
8X-5, 84.5	685.25	0.235	1.14	1.35	0.00190	0.87	0.1172	0.1026	-126	0.0576	0.0371	-0.06679261
8X-5, 88	688.00	0.544	0.58	3.13	0.00252	0.50	0.0914	0.0459	-233	0.0247	0.0477	-0.05569615
8X-5, 106	707.00	0.849	2.86	0.46	0.00317	1.11	0.0462	0.0512	-45	0.0336	0.0230	-0.03984628
8X-5, 116	717.00	0.359	2.72	0.46	0.00322	1.12	0.0463	0.0517	-40	0.0304	0.0218	-0.035460655
8X-5, 126	727.00	1.378	3.07	0.37	0.00319	1.13	0.0469	0.0531	-37	0.0301	0.0203	-0.03366359

Note: Depth refers to depth in Core 171B-1049C-8X.